Surrogate Pheromone Plumes in Three Forest Trunk Spaces: Composite Statistics and Case Studies

Harold W. Thistle, Holly Peterson, Gene Allwine, Brian Lamb, Tara Strand, Edward H. Holsten, and Patrick J. Shea

ABSTRACT. An atmospheric tracer gas was used as a pheromone surrogate to study near-field canopy dispersion within the trunk space. The objective is to improve guidance for forest managers deploying bark beetle antiaggregation pheromone sources to protect high-value forest stands. Data are shown from field studies in three forest canopies (oak-hickory, *Quercus-Carya*; lodgepole pine, *Pinus contorta* Dougl. ex Loud.; and ponderosa pine, *Pinus ponderosa* Dougl. ex Laws.) and include over 13,000 chemical tracer samples compiled into half-hour dispersion fields around a point source. Maximum normalized concentrations (χ/Q) at each arc distance for each sampling period were of similar order at 5 m from the tracer source in the three canopies, although the differences in maximum χ/Q between canopies increased with distance from the source. Plume dilution was highest in this study in the more open ponderosa pine canopy. A high-frequency tracer gas analyzer was also deployed to ascertain the structure of the gas plumes at 1 Hz. The high-frequency tracer data showed that the 30-minute average mean plumes are composites of narrow filamentous plumes. The near-field plumes in each canopy were strongly affected by changes in atmospheric stability, as wander range and meander frequency increased after the morning transition to an unstable boundary layer. FOR. SCI. 50(5):610–625.

Key Words: In-canopy dispersion, bark beetle, dispersion fields.

IN THE PAST FEW DECADES, outbreaks of North American bark beetles have brought about renewed interest in these devastating forest pests. The impact of these outbreaks and the anticipated impact of future outbreaks have stimulated the continuation of basic and applied research on the use of semiochemicals to manipulate bark beetle populations (Werner and Holsten 1995).

Bark beetle semiochemical communication systems are complex, involving insect physiology, pheromone chemistry, and microclimate processes in the forest stand. There have been many successful applications of semiochemicals to manage bark beetles as well as many failures (Shea et al. 1992, Amman 1993, Borden 1995). Inconsistency in semiochemical application effectiveness could lead to a

Harold W. Thistle, Program Manager, USDA Forest Service, FHTET, 180 Canfield St., Morgantown, WV 26505—Phone: (304) 285-1574; Fax (304) 285-1564; hthistle@fs.fed.us. Holly Peterson, Professor, Montana Technical University, Department of Environmental Engineering, 1300 West Park, Butte, MT 59701—Phone: (406) 496-4339; hpeterson@mtech.edu. Gene Allwine, Research Associate, Brian Lamb, Professor, and Tara Strand, Graduate Assistant, Washington State University, Department of Civil and Environmental Engineering, Pullman, WA 99164-3140—Phone: (509) 335-5702; blamb@wsu.edu. Edward H. Holsten, Research Entomologist, USDA Forest Service, 3301 "C" St., Suite 202, Anchorage, AK 99503-3956—Phone: (907) 743-9453; eholsten@fs.fed.us. Patrick J. Shea, Emeritus Researcher, USDA Forest Service, 1107 Kennedy Pl. #8, Davis, CA 95616—Phone: (530) 758-5078; pjshea@davis.com.

Acknowledgments: The authors acknowledge the contribution of Dr. Richard Reardon for his ongoing technical support, Patricia Skyler, Mike Huey, Wes Throop, Robert Beckley, and Jaris Brey for their assistance in the field, and Sandy Fosbroke for her assistance in preparation of this document. This work is supported under USDA Forest Service Projects FHTET TD.00.M03 and FHTET TD.00.M01.

Manuscript received May 23, 2003, accepted March 30, 2004

reluctance of manufacturers to produce semiochemicals for operational uses and could cause forest pest managers to be hesitant to use these chemicals for pest management strategies (Borden 1995). These failures could be caused by technical problems involving deployment, consistent release, and longevity of releasers as well as the influence of the microclimate within the stand. Holsten and others (2002, 2003) have addressed technical problems associated with pheromone releasers and demonstrate the dependence of the pheromone release rate on microclimate and exposure. The following study addresses the in-canopy dispersion of pheromone plumes.

This tracer test program evaluated in-canopy pheromone dispersion and was conducted over 4 years; field data were collected during June 1998 in a managed ponderosa pine (*Pinus ponderosa* Dougl. ex Laws.) canopy, Aug. 1999 in an eastern oak-hickory (*Quercus-Carya*) canopy, July 2000 in a lodgepole pine (*Pinus contorta* Dougl. ex Loud.) canopy, and June 2001 in an additional ponderosa pine canopy. Sites were selected both to measure tracer dispersion in bark beetle habitat and to provide a range of canopy types to ascertain canopy influences on the dispersion environment. The first study year was conducted with limited instrumentation and is described elsewhere (Thistle et al. 1999). This article summarizes results from the three field seasons from 1999 to 2001. From a process standpoint, the system under investigation can be approached as consisting of three components: a source of the pheromone gas, a dispersion field around the source, and the interaction of the pheromone gas with insect physiology influencing insect behavior. This study addresses the second aspect of this system and describes the dispersion environment in the lower forest canopy where bark beetle pheromone pest control strategies are generally implemented. A tracer field program is described in this article, and patterns of mean concentration as well as results from high-frequency analysis of tracer gas concentrations are presented.

Background

Mechanisms of pheromone action are specific to the insect and the specific pheromone being studied. However, the dispersion of any gaseous scalar quantity under a canopy can be treated generically by assuming chemical passivity (assuming no in-canopy sinks of pheromone) as a first approximation. Dispersion of the gas is then largely determined by meteorology and canopy density and distribution. The micrometeorology in plant canopies is complex due to the three-dimensional, porous nature of canopies, the highly turbulent flow environments in canopies, and the wide diversity of canopy density and architecture (see overviews by Kaimal and Finnigan [1994] and Finnigan [2000]). LeClerc et al. (2003a) used SF_6 to study the flux of tracer vertically out of a peach orchard and in a separate study from a mature southern pine canopy (LeClerc et al. 2003b). Staebler (2003) investigates horizontal advection of CO_2 in-canopy and the coupling (or lack thereof) of the in-canopy flow with the above canopy atmosphere.

Some earlier work on the pheromone dispersion problem focused on mating disruption of gypsy moth (Aylor et al. 1976, Elkinton et al. 1984). Fares et al. (1980) proposed a Gaussian model for pheromone dispersion in a forest based on biological data. Insect mating disruption studies are ongoing in agricultural settings (Carde et al. 1998) and have led to fundamental work on plume tracking mechanisms (Li et al. 2003). Farrell et al. (2002) created a model of the high-frequency dispersion of pheromone plumes. The use of tracer gases as surrogates to study pheromone plume movement in canopies is not novel (Murlis and Jones 1981), although the density of the data array and the combination of high- and low-frequency sampling in the canopy trunk space in our work yield a unique data set. There are few estimates of the effective radius of a pheromone source in the literature. Schlyter (1992) gave an approximate attraction range for Lepidoptera of 200–400 m, but bark beetle attraction ranges were typically much lower (<100 m, dependent on species). Turchin and Odendaal (1996) used a trapping grid to determine the percentage of recaptured beetles released at known distances from a given attractant source. Recapture rates varied from around 0.01% at 900 m to around 10% at 10 m. Dodds and Ross (2002) showed recapture rates of over 90% at less than 200 m from the pheromone source in Douglas-fir beetle (*Dendroctonus pseudotsugae*). These rates decreased sharply over 200 m.

Methods

The tracer gas chosen for this work is SF_6. This is an industry standard tracer with minimal toxicity that can be detected at very low concentrations and is chemically inert and conservative over the time scales of an experimental trial (4.5 h). There is extensive literature describing the use of SF_6 as a tracer in various settings (Guenther et al. 1990, Thistle et al. 1995, Allwine et al. 2002, and many others). Theoretically, the emission of a gas from a source will scale linearly with the concentration field if the gas is chemically passive and does not transform in the atmosphere or preferentially adhere onto surfaces. SF_6 fulfills these requirements, but a given pheromone may not. Therefore, the approach is to measure these tracer plumes assuming they are chemically conservative; this provides a conservative endpoint for the trunk space plumes. The pheromone plumes can then be scaled to the correct emission rate. If the pheromone is chemically depleted through transformation or adsorption onto the canopy and the ground surface, this depletion can be accounted for if it can be characterized. SF_6 has an atomic weight of 146, and although this may be larger than many pheromone molecules, the property of a well-mixed gas that affects dispersion is its bulk density. In this experiment, the SF_6 is released as a 1% mixture and is quickly dispersed to a much lower percentage in the air; therefore, buoyancy effects due to molecular properties are negligible. Slumping of the release due to expansional cooling of the pressurized gas was not observed. Thus, the tracer acts as a reasonable surrogate for the pheromone plumes. It is possible that both the introduced and natural pheromone plumes may be released at high enough concentrations that

some initial buoyancy effects may occur, but these should be rapidly dissipated through mixing.

Tracer Sampling Technology

Automated, portable samplers were used to collect air samples in polyethylene syringes (Krasnec et al. 1984). These samplers used a timer and mechanically pulled open a syringe over a half-hour period. Each sampler was built to collect nine sequential samples, and there were 50–60 of these samplers available for each test. Samplers were immediately retrieved following each 4.5-hour test, and all of the syringe samples were analyzed at a nearby field laboratory within 24 h of collection. A continuous SF_6 analyzer using electron capture detection (Benner and Lamb 1985) was employed for rapid sample analysis (Allwine et al. 1992). A second continuous analyzer was mounted in a small cart and connected to a personal computer data acquisition system to enable continuous SF_6 measurements at selected fixed points during each of the tracer tests. The analyzers are calibrated frequently using standard gasses with a certified accuracy of ±5%. The frequency of calibration is dependent on the concentration of the gas being sampled. Each instrument has a detection range of approximately 10 ppt to 10 ppb (6×10^{-8} g/m^3 – 6×10^{-5} g/m^3). The lower end of the reliable quantification range is approximately 20 ppt (1.2×10^{-7} g/m^3). The precision of repeated analyses is approximately 10%, which yields an overall uncertainty of approximately ±12% calculated as the square root for the sum of the squares of the contributing terms. The real-time analyzer yields data at around 1 Hz, and although the insect response may be >10 Hz (Mafra-Neto and Carde 1994), the temporal resolution of the real-time data overlain with the mean (half-hourly average data) yields significant insight into the question of plume structure and meander (Peterson and Lamb 1992, 1995).

Meteorological Monitoring

Mean wind vector and turbulence data were collected on the site using three-axis, 15-cm pathlength, Vx probe sonic anemometers (ATI, Longmont, CO) collecting data at 20 Hz in the 1999 field program and 10 Hz in 2000 and 2001. The sonic anemometers were deployed in a profile with one in the trunk space, one near the vertical canopy density maximum, and one above canopy. The absolute heights varied from site to site but typically ranged from 2 m in the trunk space to 28 m. A fourth sonic anemometer was collocated with the source. In the 1999 oak-hickory trials, a waving branch destroyed the midlevel anemometer, and no anemometer was deployed at the source. Two 7-m meteorological towers were also deployed, and mean meteorological data, including two levels of temperature and humidity (R.M. Young, Model 41372/43372, Traverse City, MI), wind speed and direction (MetOne, Models 5431, 024, 010C, Grants Pass, OR), and net radiation (R.E.B.S, Seattle, WA) were collected.

Sampling

A set of three concentric circles with 5-, 10-, and 30-m radii centered on the emission point was marked for sampler deployment. The 5-m radius circle had 12 possible sampling locations, one every 30 degrees. The 10- and 30-m radius circles had 24 possible sampling locations each, one every 15 degrees. Each sampling location was identified with a circle radius and an azimuth angle. The basic mean sampler array was deployed at 1.2 m above ground. This results in a very dense horizontal array and allows evaluation of horizontal dispersion in the canopy trunk space. Bark beetle attacks occur in the trunk space well below the level of maximum foliage density. Thus, plume sampling is focused in this canopy sublayer. Elevated sampling to determine vertical dispersion coefficients as well as the vertical scalar flux in the canopy was conducted. A high tower had three sampling stations distributed vertically from 1.5 m to the maximum height of approximately 28 m. Various elevated sampler arrays on other, shorter sampler towers were employed over the course of the studies. Between 50 and 60 samplers were available for a given test so the total number of samplers varied, but at least 12 samplers were hung on both the 5 and 10-m arcs at 1.2 m in height for each test. The rest were either deployed at a different height or were used to increase the sampling density at 1.2 m on the 10 and 30-m arcs. The samplers were programmed to start simultaneously at all sampling locations. The sampling period was set for 30 minutes per sample, and each test was 4.5 hours in duration. Background concentrations of SF_6 can be above detectable levels, so background concentration levels were monitored. As described above, one continuous SF_6 analyzer was deployed in each trial. This instrument was positioned based on mean wind indications, and the inlet port was located at the closest marked array position at a 1.2-m height typically on the 10-m arc. This analyzer was moved if the wind changed, but generally the analyzer was kept at a fixed point for at least 30 minutes.

Site and Canopy Description

Site locations are given in Table 1. Locally level sites were chosen, alhough some slope was accepted as typical of management scenarios. Leaf Area Index (LAI) is defined as the projected unit leaf area (one-sided) per unit ground area normal to the slope. Leaf area measurements were made over the three field seasons using two methods. The first method used the LI-COR 2000 Plant Canopy Analyzer (LI-COR, Inc., Lincoln, NE). Due to concerns about the accuracy of the Plant Canopy Analyzer (PCA), especially in coniferous canopies, a Hemispherical Photographic Technique (HPT) was also used. Leaf area was measured at approximately 60 points from the ground in each of these canopies. The PCA tended to underestimate leaf area in coniferous canopies and generally gave larger leaf area values than the HPT in the deciduous canopy (Throop et al. 2001). The three test canopies are described in Table 1. Deciduous canopies are more likely to fulfill the operational requirements of the PCA instrument because the deciduous overstory is typically more spatially uniform and has fewer large gaps that allow directionally oriented illumination under the canopy. The two instruments agree within about 1.2 m^2m^{-2} one-sided LAI in the oak-hickory canopy. The lodgepole pine canopy was the densest in terms of stems per

Table 1. Project site location and basic canopy metrics for the three trial seasons.[a]

Location	Date	Elevation (above sea level) (m)	Canopy type	Average canopy height (m)	Stems per hectare[b]	PCA average LAI	Standard deviation PCA	Range PCA	HPT average LAI	Standard deviation HPT	Range HPT
Goshen, VA 37°55′09″ N 78°29′40″ W	August 1999	568	Oak-hickory, mixed forest	21	665	3.58	0.78	2.4–5.4	2.38	0.44	1.7–4.1
Potomac, MT 46°54′19″ N 113°126′45″ W	July 2000	1,207	Lodgepole pine	30	1,521	2.18	0.70	0.8–3.3	2.50	1.15	1.0–6.1
LaPine, OR 43°48′08″ N 121°39′34″ W	June 2001	1,447	Ponderosa pine	35	389	1.8	0.47	1.1–3.2	3.3	0.98	2.1–6.4

[a] Canopy one-sided LAI (leaf area index, m^2m^{-2}) summary statistics as collected using the plant canopy analyzer (PCA) and the hemispherical photographic technique (HPT).
[b] Stems greater than 7.6 cm dbh.

acre and was fairly uniform. This canopy offered the best agreement between the PCA and HPT methods. The ponderosa pine canopy is not well described using LAI because it is characterized by large gaps between trees and is not an ideal candidate canopy for either of these measurement methods but is probably better suited to the HPT. Published values of LAI using more sophisticated measurement techniques conducted in ponderosa pine in the same geographical area are similar to those presented in Table 1 (Law et al. 2001).

Results and Discussion

Concentration versus Distance

The basic result of this study is a compilation of normalized concentration (χ/Q [sm^{-3}], where χ is concentration [gm^{-3}] and Q is the source emission rate of SF_6 [gs^{-1}]) plotted against distance from the point source of tracer. These data allow managers to begin to understand the concentrations of the pheromone gas in the forest stand surrounding the release point. The data set consists of 243 sampling periods, consisting of 50–60, 30-minute average chemical samples per period. The average data from each period can be viewed as a realization of the concentration field around the source. There is a maximum average value of χ/Q on each sampling arc (5, 10, and 30 m) for each period. The aggregate analyses presented are based on the maximum χ/Q for each period. There are 81 maximum values (one per 30-minute average sampling period) for each arc for each canopy type (minus a few in some of the analyses; for instance, the sonic anemometer data was not considered good in the rain, although the mean chemical data was). This leads to discussion of "highest maximum χ/Q" and "lowest maximum χ/Q" at each arc for a given canopy.

A coarse mass balance exercise was performed with a 10-trial subset of the data from the ponderosa pine canopy and the lodgepole pine canopy (Thistle et al. 2002). The mass balance exercise ratios the mass of source material released with the amount of material recovered at a given arc distance. A ratio approaching unity indicates the sampling scheme is correct. This ratio is often far from unity in environmental studies. Mass balance was within a factor of two in 90% of the tests, with the best result for the subset from the ponderosa pine showing an arithmetic average mass balance of 1.04. It is anticipated that with refined assumptions, the mass balance numbers will improve. This exercise yields substantial confidence in the experimental data.

The 30-minute average concentrations were normalized to remove the effect of varying source strength (the emission rate of the pheromone is referred to as an elution rate). Figure 1,a–c shows the range of arc maxima χ/Q for the three field sites. In the oak-hickory stand (Figure 1a), the median values of the arc maxima χ/Q ranged from 0.15 at 5 m through 0.075 at 10 m and 0.012 at 30 m. This shows the expected decrease in concentration with distance, as χ/Q fell by half at 10 m and was about 8% of the 5 m value at 30 m. If the range of χ/Q is viewed as (highest max

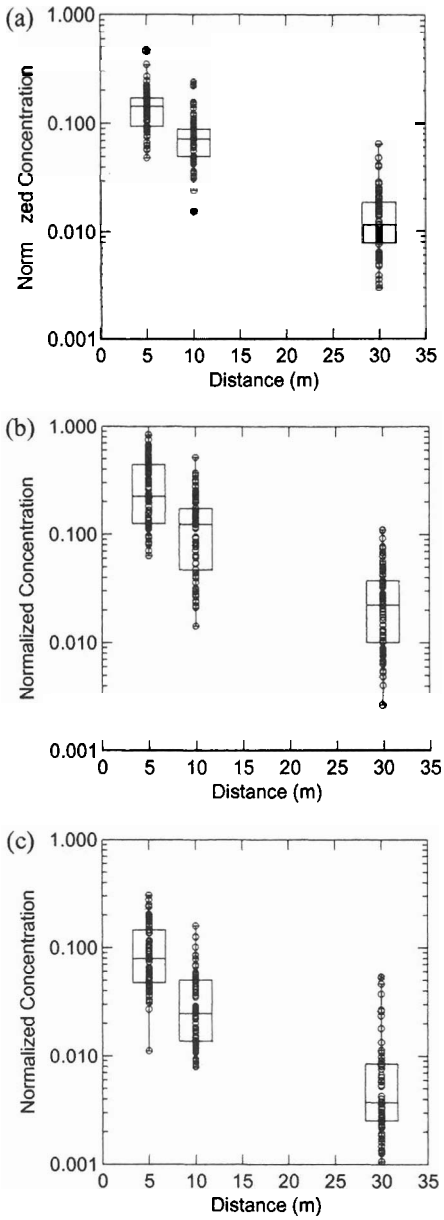

Figure 1. Normalized concentration maximum (χ/Q) values on each arc for the entire 81 half-hours for the (a) oak-hickory canopy, (b) lodgepole pine canopy, and (c) ponderosa pine canopy. Note the middle horizontal line of the box-plot indicates the median value, and the upper and lower limits of the box represent first and third quartiles.

χ/Q)/(lowest max χ/Q) on a given arc, this value increased from around 10 at 5 m to 12 at 10 m, and close to 25 at 30 m. Thus, there was substantial variation in χ/Q along each arc among all of the tests in this canopy, and this variation increased with distance from the source.

As shown in Figure 1b, median values of maximum χ/Q in the lodgepole pine stand at the given arcs were 1.5–2 times higher (0.22 at 5 m, 0.12 at 10 m, and 0.025 at 30 m) than those in the oak-hickory stand (Figure 1a), although they showed a very similar relationship with distance (the 10-m value was about half the value at 5 m, and the 30-m value was approximately 10% of the 5-m value). However, the range of χ/Q was much greater in this canopy compared with the oak-hickory stand, showing a factor of 15 at 5 m increasing to near 50 at 10 and 30 m.

In Figure 1c, the χ/Q arc maxima values in the ponderosa pine stand are much lower than in the other two stands. The median values ranged from 0.08 at 5 m through 0.023 at 10 m and 0.0035 at 30 m. These values also showed a high range factor (30, 26, and 60 at 5, 10, and 30 m, respectively) though not dissimilar to that in the lodgepole pine stand. A distinguishing facet of these stand data is that the arc median maximum χ/Q at 30 m was around 4% of that at 5 m, indicating a more rapid dispersion of the material. The 30-m median value was about one-quarter of that at 30 m in the oak-hickory stand.

Concentration versus Wind Speed

It is expected that a basic relationship will exist in these data between the mean wind speed and maximum arc concentration. As the wind speed increases, more air is introduced into the plume and the plume becomes more dilute. This is a simplistic conceptualization in the environment as these data show, but it provides an insightful starting point and generally proves to be relatively robust. This relationship exists in some of these data but is weak in much of it as seen in Figure 2. The relationship shown in Figure 2a for the oak-hickory canopy may be explained by the very low range and low absolute value of wind speed experienced during this trial. The half-hour average wind speeds in the lower trunk space were between 0.1 and 0.7 m/s for all 81 half-hour periods measured in the oak-hickory canopy. This points out the very low wind speed environment often encountered in the trunk space of leaved deciduous canopies. With this said, the graph shows the expected tendency, but the relationship is weak.

The lodgepole pine canopy shows the expected relationship with wind speed more strongly than the other two canopies, although the relationship is still noisy (Figure 2b). This canopy had a larger range of wind velocities during the tests due mostly to what appeared to be mesoscale density flows related to regional slopes. The relationship appears to be weak (between 0.2 and 0.4 m/s), but then concentration drops off more coherently as wind speed increases beyond that.

The ponderosa pine canopy shows weak correspondence between wind speed and concentration even though the range of wind speed was relatively high (Figure 2c). This graph gives the impression that the expected relationship may exist in some cases but is influenced by outliers. This canopy had fewer trunks than the lodgepole pine canopy, and specific cases of mesoscale density flows, as discussed below, were experienced, although the weather did not generally favor these during these trials.

Concentration versus Wind Direction Variance

Aggregate scatter plots of the variance of wind direction angle (σ_ϵ) versus maximum χ/Q for each half-hour period are shown. These graphs were produced for the ponderosa pine and lodgepole pine data sets using the sonic anemometer collocated with the tracer source. There are various

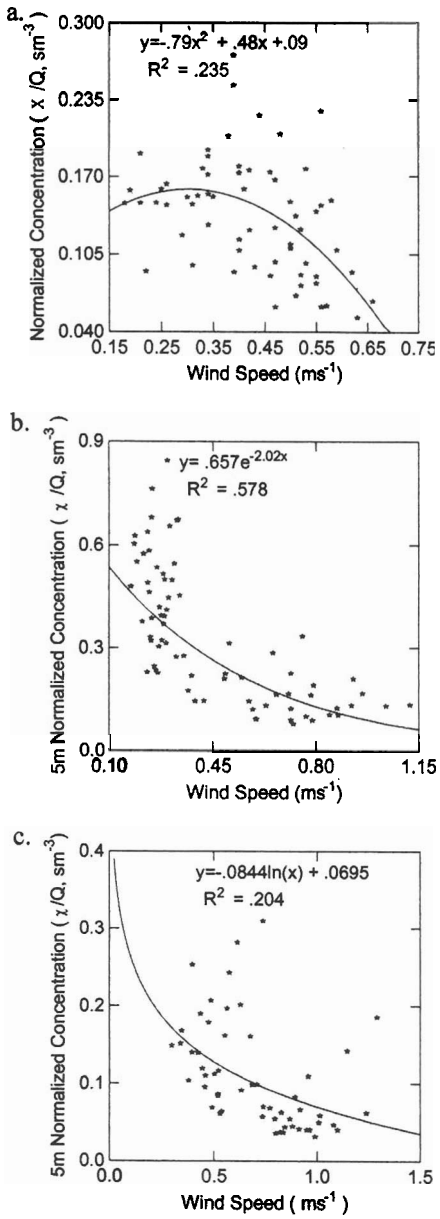

Figure 2. The relationship between the 30-min maximum χ/Q values at the 5-m horizontal sampler arc and the mean wind speed in the (a) oak-hickory canopy, (b) lodgepole pine canopy, and (c) ponderosa pine canopy.

ways to calculate directional variance; here it is simply expressed as

$$\sigma_\epsilon = (v/U) \qquad (1)$$

and expressed in radians. Here v is the 30-minite average lateral variance in the wind speed (ms^{-1}, and U is the rotated 30-minute vector average (ms^{-1}); both quantities were measured at the source sonic anemometer. The sonic anemometer coordinate system is fixed and the raw data are rotated into the predominant wind direction so U is the average velocity in the mean direction and the average mean lateral direction (V) is forced to zero (see Wilczak et al. 2001 for a complete discussion of sonic anemometer coordinate transforms).

It is expected that the concentration field will vary with σ_ϵ because as the direction varies, the plume covers a wider area laterally but is at each receptor a smaller percentage of the sampling period. It is expected that maximum χ/Q will decrease as σ_ϵ increases, and this trend is generally seen in these data. In the lodgepole pine canopy, this relationship is seen, but the scatter plot shows two regions. The pattern seen in Figure 3a shows a transition value of χ/Q around 0.2. Below this value, σ_ϵ ranges from around 0.1 to 0.7. Above 0.2, σ_ϵ only ranges from around 0.2 to 0.4. In the ponderosa pine canopy (Figure 3b), the range of χ/Q is much lower, and although the basic relationship of decreasing χ/Q with increasing σ_ϵ is seen, the relationship shows large scatter.

Concentration versus Atmospheric Stability

It is well known that the vertical temperature structure (stability) in the atmospheric layer that is transporting a gaseous quantity has a strong influence on dispersion (Kaimal 1973, Kaimal et al. 1976, Thistle 2000, and many others). In the atmospheric layer under the canopy, hydrostatic pressure changes due to changes in height are small because the layer is only tens of meters thick, so stability is reasonably determined by the absolute temperature difference across the canopy layer. If temperature increases with height, the layer is stable and vertical mixing is damped; if temperature decreases with height, the layer is unstable and vertical mixing is enhanced. A common measure of the

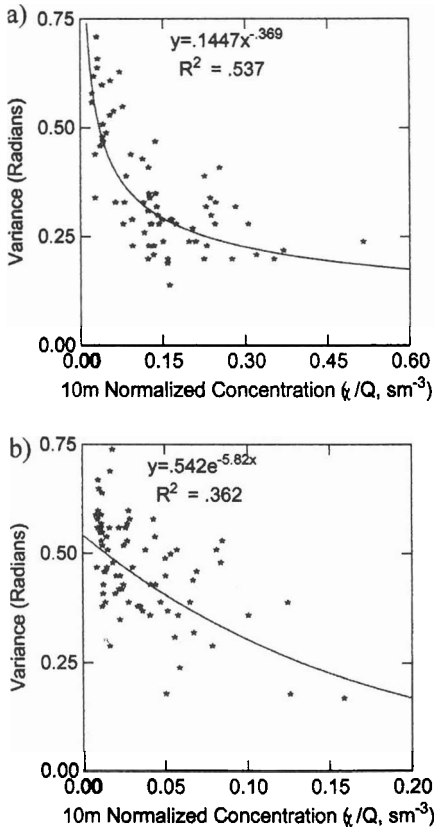

Figure 3. Variance (v/U) plotted against 30-min maximum χ/Q (a) at the 10-m arc in the lodgepole pine canopy and (b) at the 10-m arc in the ponderosa pine canopy.

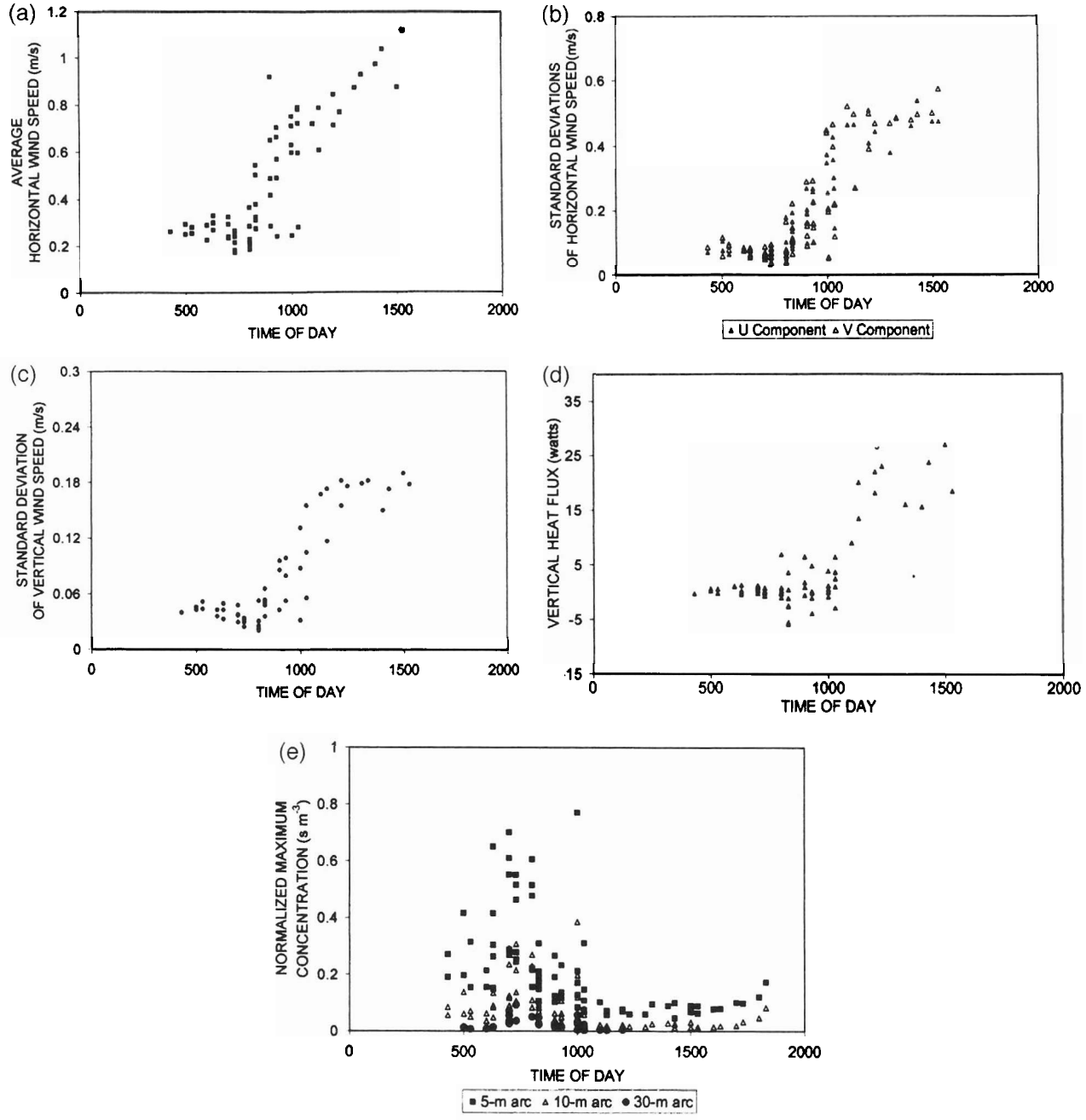

Figure 4. Lodgepole pine canopy. (a) Average horizontal wind speed at the tracer source plotted against time of day. (b) Standard deviation of horizontal wind speed at the tracer source versus time of day. (c) Standard deviation of vertical wind speed at the tracer source plotted against time of day. (d) Vertical heat flux at the tracer source plotted against time of day. (e) Normalized maximum concentration plotted against time of day as a function of sampling arc.

influence of buoyant forces on vertical mixing is the Richardson Number:

$$Ri = g/T_a\,((\Delta T/\Delta z)/(\Delta U/\Delta z)^2 \qquad (2)$$

In this study, Ri was calculated for the lodgepole pine and ponderosa pine canopies using the differences in U and temperature (T, °K) between the lowest sampling station and the middle station on the high tower; g is the acceleration of gravity (ms^{-2}), and T_a is the layer average temperature (°K) over the vertical layer Δz (Δz = 12.8 m in the lodgepole pine canopy and 12.0 m in the ponderosa pine canopy). The Ri was difficult to correlate to χ/Q due both to the fact that very low values of dU/dz made the ratio numerically unstable and the physical problem that in morning transitions the vertical structure of T is complicated as the solar radiation is initially intercepted in the upper canopy. This can cause T to increase sharply with height for a brief period. The strongly stable layer in the trunk space that develops as indicated by Ri is not necessarily reflected in sharp increases in maximum χ/Q. This is probably because the mixing environment in the trunk space is not changed until the surface is illuminated or larger scale atmospheric

convection mixes air into the trunk space later in the morning transition.

The relationship of mixing in the trunk space to stability is best illustrated by the lodgepole pine data. Much of the ponderosa pine data was collected in neutral atmospheric conditions and the oak-hickory data suffered from instrument limitations as well as less variation in stability. In the lodgepole pine data set, every morning trial saw a dramatic change in regime from cool, clear, still early conditions to hot, gusty, sunny conditions later in the day. In this regularly repeating weather regime, both meteorological statistics and the tracer dispersion correlated strongly with time of day; that is to say, that as the atmospheric surface layer transitioned from a relatively shallow, stable layer to a deep, convectively mixed layer, the dispersion environment in the lodgepole pine trunk space reflected this change as χ/Q decreased. Figure 4, a–e reflects this transition. Early in the day, wind speeds are low, variance of the wind statistics is low (reflecting suppressed mixing), heat flux is low, and χ/Q is high, reflecting the low mixing environment. Later in the day, the wind speeds increase, turbulence increases as reflected in the increase in the wind speed variance statistics, vertical mixing increases as increased heat flux instigates convective mixing, and χ/Q decreases.

A strong outlier in Figure 2c shows high maximum χ/Q (0.305 sm^{-3}) at relatively high U (0.74 ms^{-1}). This occurred in the 30-minute period beginning at 0430 when the mean wind speed profile was inverted so that the winds near the surface were higher velocity than those at the canopy top. This is caused by a shallow drainage flow occurring near the surface, indicating the plume was in a stable, low-mixing environment although the drainage flow was relatively high velocity.

Discussion of Mean Aggregate Dispersion and Stand Density

The dispersion data (Figure 1) show pheromone dilution rates for different types of canopies. In Figure 5, median χ/Q are shown as a function of stem density for each downwind distance (values in Figure 5 are significantly different at $P \leq 0.05$). Figure 5 provides the first step toward an empirical method of guiding the placement of pheromone sources. Using this plot, diagrams could be developed to show dilution levels as a function of source spacing and stem density. In turn, information will be needed that includes the pheromone levels to which the insect responds and the rate at which specific pheromone release devices elute pheromone such as described by Holsten et al. (2002). It is important to note, however, that the patterns shown in these figures reflect not only stem density effects but also depend on the meteorology experienced during each field program.

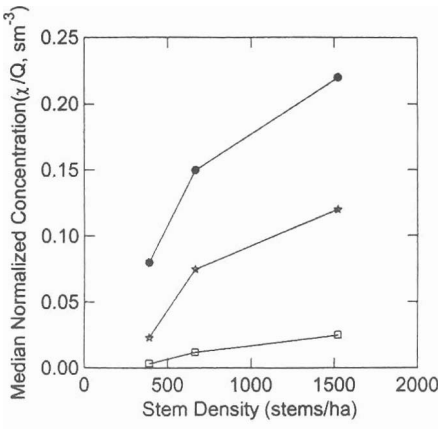

Figure 5. Median of maximum normalized concentration versus stem density for different distances from the source.

The vertical distribution of the drag of the oak-hickory canopy and the lower wind speeds experienced during these tests influence the relationship between dispersion and wind speed in that canopy. The drag is larger in the foliage in the upper reaches of the canopy and may act like a filter, breaking higher velocity gusts into less energetic, smaller-scale turbulence as the foliage dissipates momentum. In the lodgepole pine canopy, the structure of the canopy can be qualitatively described as a hairbrush with a large part of the drag provided by the narrow lodgepole pine trunks as opposed to flat, flexible deciduous leaves. Drag is therefore distributed more evenly through the lodgepole pine canopy as opposed to the drag in the deciduous canopy, which is largest near the canopy top. This structure may allow higher velocity gusts to penetrate into the canopy and the mean flow to be less intermittent. The ponderosa pine canopy structure is intermediate between the other two. The trunks are more widely spaced than in the lodgepole pine, but the canopy drag elements are more evenly distributed with height than in the oak-hickory canopy.

Canopy Top Tracer Venting

A mean SF_6 sampler was raised into the upper canopy in each test. Table 2 indicates sampler positions on the high tower. Because the high tower was at a fixed location, there were many trials when the wind direction determined that no material reached the high tower samplers. Also, the act of hoisting the samplers up the tower caused a lower percentage data recovery from the high samplers due to rough handling and the difficulty of checking the samplers after deployment. This leaves a limited number of typically low concentration samples to base conclusions on. These considerations make this discussion somewhat qualitative.

Even at this relatively short source-to-sampler distance, there was tracer seen at the high samplers. In the lodgepole pine canopy, only one trial showed nonzero tracer concentrations. (Zero accounts for background SF_6 levels that are currently around 3 ppt globally. Background measurements were made during all trials and generally showed background concentrations less than expected and near true zero; this is probably due to the rural nature of these sites.) However, the oak-hickory and ponderosa pine canopies showed nonzero concentrations at the highest samplers during 42 and 15% of trials where data were recovered at the highest sampling location, respectively. Figure 6, a and b shows vertical profiles when the top sampler was nonzero. The very low values for the lodgepole pine canopy are

Table 2. Positioning of high tower samplers.

Test canopy	Horizontal distance (m)	Mid-level sampling height (m) (scaled height[a])	Top sampling height (m) (scaled height[a])
Oak-hickory	20	13.8 (0.66)	26.7 (1.27)
Lodgepole pine	20	14.5 (0.48)	24.9 (0.83)
Ponderosa pine	28	13.3 (0.38)	26.5 (0.76)

[a]Scaled height = sampler height divided by average canopy height.

believed to be due to the fact that the regular weather pattern that predominated during the tests (as discussed above) was typified by low wind speeds with little mixing early and then a stronger flow that indicated a regional upslope flow. Although the upslope flow, indicating a transition to an unstable atmosphere, did increase mixing, the mean directional component was away from the tower. The high frequency of nonzero detection above the oak-hickory stand is interesting and may simply be due to the low wind speed conditions and the opportunity for the tracer to diffuse upward before being transported below the tower samplers horizontally. In the ponderosa pine canopy, the top sampler was well below the average tree height, so the sampler may be thought of as in the canopy, although this canopy is not closed because the upper canopy is composed of individual conical treetops. Because the tower was further from the source in the ponderosa pine trials, the material had more time to diffuse upward but is also more dilute. It must also be pointed out that the levels detected at the top sampler in the ponderosa pine canopy were very low and often approached the detection limit. These measurements indicate a small amount of tracer was present, but the absolute values fall within the measurement error range. It can be concluded that even within 20–30 m of the source, some tracer material exits the canopy vertically.

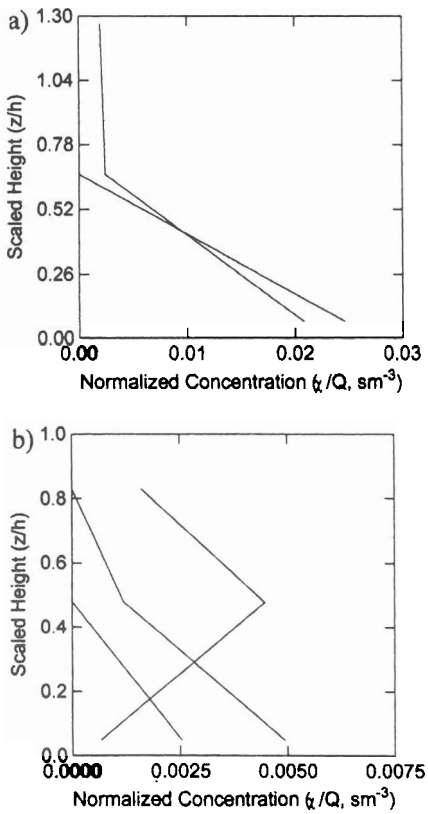

Figure 6. Examples of vertical profiles of 30-minute χ/Q from the high sampling tower in the (a) oak-hickory canopy and (b) lodgepole pine canopy.

Case Studies

Selected periods are shown to illustrate the nature of the movement of the tracer in the canopy trunk space. High-frequency data are shown to illustrate the nature of the dispersion at 1 Hz and to compare with half-hour averages of concentration. Use of these high-frequency data is conditioned by the fact that this is a stationary, single-point measurement made at a 1.2-m height at the position indicated. As such, these time series of χ/Q show the passage of the plume. The sensor may be in the plume for an extended period or the plume may meander across the sensor (or the side or bottom and so forth of the plume may touch the sensor port). Therefore, these high-frequency series must be carefully interpreted. Generally, if multiple peaks of similar magnitude are measured within some time frame, it is assumed that these concentrations represent centerline concentration. Furthermore, as individual measurement periods are examined, it is useful to individually fit Gaussian curves. This curve fitting is the first step in allowing other dispersion modelers to extend into the trunk space using existing techniques. Strand et al. (2002) have begun model development using the tracer dispersion data collected in ponderosa pine during this study.

Isopleth plots are shown to facilitate visualization of the concentration field. These plots are created using a distance weighted least squares (DWLS) algorithm (Systat 10; SPSS, Inc., Chicago, IL); the contour interval is evenly divided between the maximum value of χ given in the caption and zero. Assumptions made to produce these plots make them suitable for conceptual purposes, but they should not be used for detailed metrics. The field study was adjusted continually, although the primary changes occurred between field seasons. This results in some differences between the analyses that can be performed from season to season. Summary data for these cases are shown in Table 3.

Oak-Hickory Canopy, 8:00 am, Aug. 27, 1999

Figure 7a shows an elongated plume along a generally NW-SE axis, although the isopleths are not smooth. This is reflected in the linearized cross sections that clearly show three peaks and a very weak Gaussian fit (Figure 7b). The

Table 3. Mean statistics of periods shown in the case studies.

Date	Start time	*Ri#*	*U* (ms^{-1})	*T* (°C)	*H* (Wm^{-2})	u'w" (m^2s^{-2})	*RH* (%)	5-m max χ/Q (sm^{-3})	10-m max χ/Q (sm^{-3})	30-m max χ/Q (sm^{-3})
Aug. 27, 1999	0800		0.25	16.1	6.4	0.0	91	0.157	0.086	0.011
July 24, 2000	0700	–447.8	0.24	9.1	0.5	-0.001	76	0.321	0.116	0.047
July 24, 2000	1030	–192.2	0.59	20.9	6.4	–0.027	35	0.084	0.04	0.008
June 21, 2001	1100	–4,478.2	1.14	24.5	14.5	–0.060	28	0.138	0.047	0.003

Ri#, Richardson Number; *U*, wind speed; *T*, temperature; *H*, heat flux; *RH*, relative humidity; χ/Q, concentration/release rate.

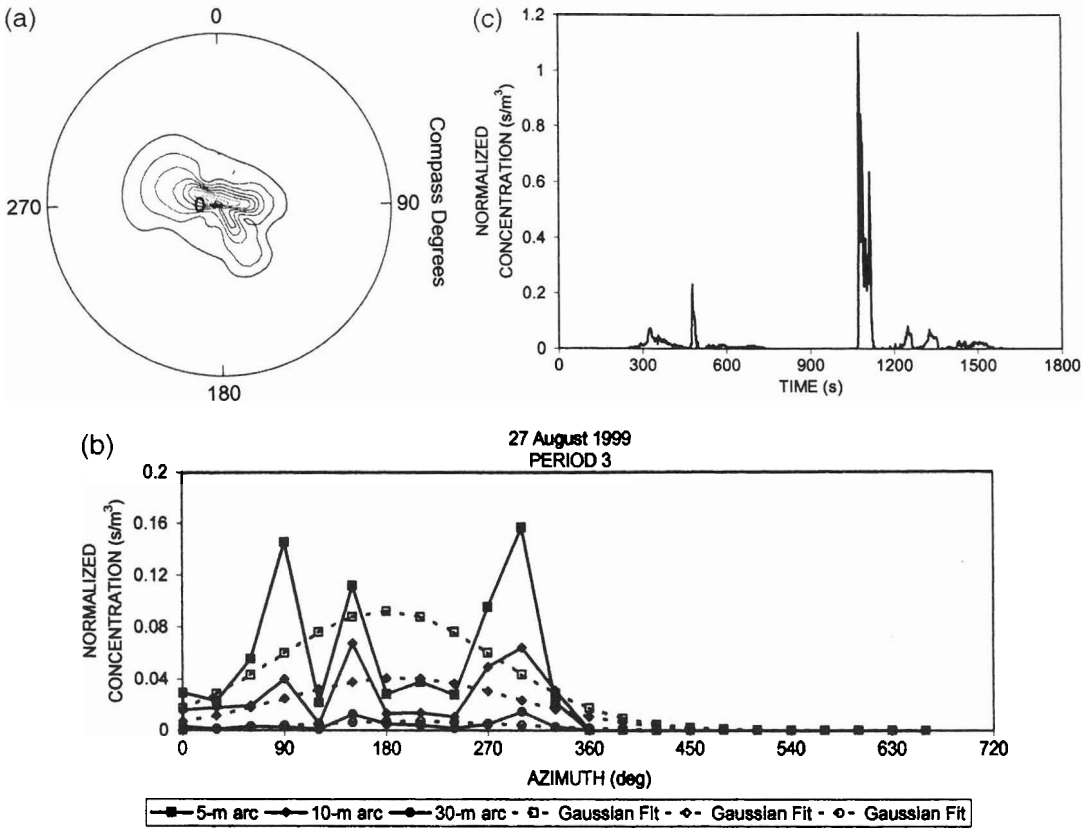

Figure 7. Aug. 27, 1999, 8:00 am case study. Oak-Hickory canopy. (a) Spatial isopleths of 30-minute χ/Q, with the maximum contour at χ/Q = 0.2 and the tracer source at the center of the concentric sampler arcs. Sampler positions are designated. (b) Linearized cross sections of 30-minute χ/Q compared with best-fit Gaussian cross sections. (c) High-frequency time series composed of 1 Hz averages of tracer χ at one point on the 10-m sampler arc.

high-frequency time series shows one discrete peak with a peak-to-mean ratio of 58.8 (Figure 7c), and even this is deceptive because far from being a mean process, the plumes (or filaments) have dramatic discrete edges that are crossed on the order of single seconds. It is interesting to note that the high-frequency plumes do appear to be amenable to Gaussian modeling, although correctly specifying the meander frequency and plume wander make correctly ensembling the high-frequency plumes into low-frequency plumes difficult. These data combined indicate a low-dispersion environment without much mean energy and a few discrete pushes of tracer movement over the half hour, only one of which crossed the high-frequency sampling point. In all of these trials, the mean half-hourly average plume is actually a manifestation of highly concentrated tracer filaments moving back and forth across the sampler field (Figure 7c). It is known that gaseous plumes have this structure and have been seen to exhibit similar structure at over 100 Hz (Yee et al. 1994), so that even the very concentrated plumes measured here at 1 Hz are composed of even finer threads with even larger peak-to-mean ratios. The work of Mafra-Neto and Carde (1994) indicates that beetles may be able to sense these plumes at >10 Hz.

Lodgepole Pine Canopy, 7:00 am, July 24, 2000

This period was characterized by high χ/Q, low heat flux, and very low wind speed. *Ri* was relatively large negative, but, as noted above, this ratio is numerically unstable when dU/dz is small as it is here. This case represents a still, clear morning, and there is very little mixing in the lower canopy. The plume shape is fairly regular, with the long axis shown on the isopleth graph (Figure 8a) also

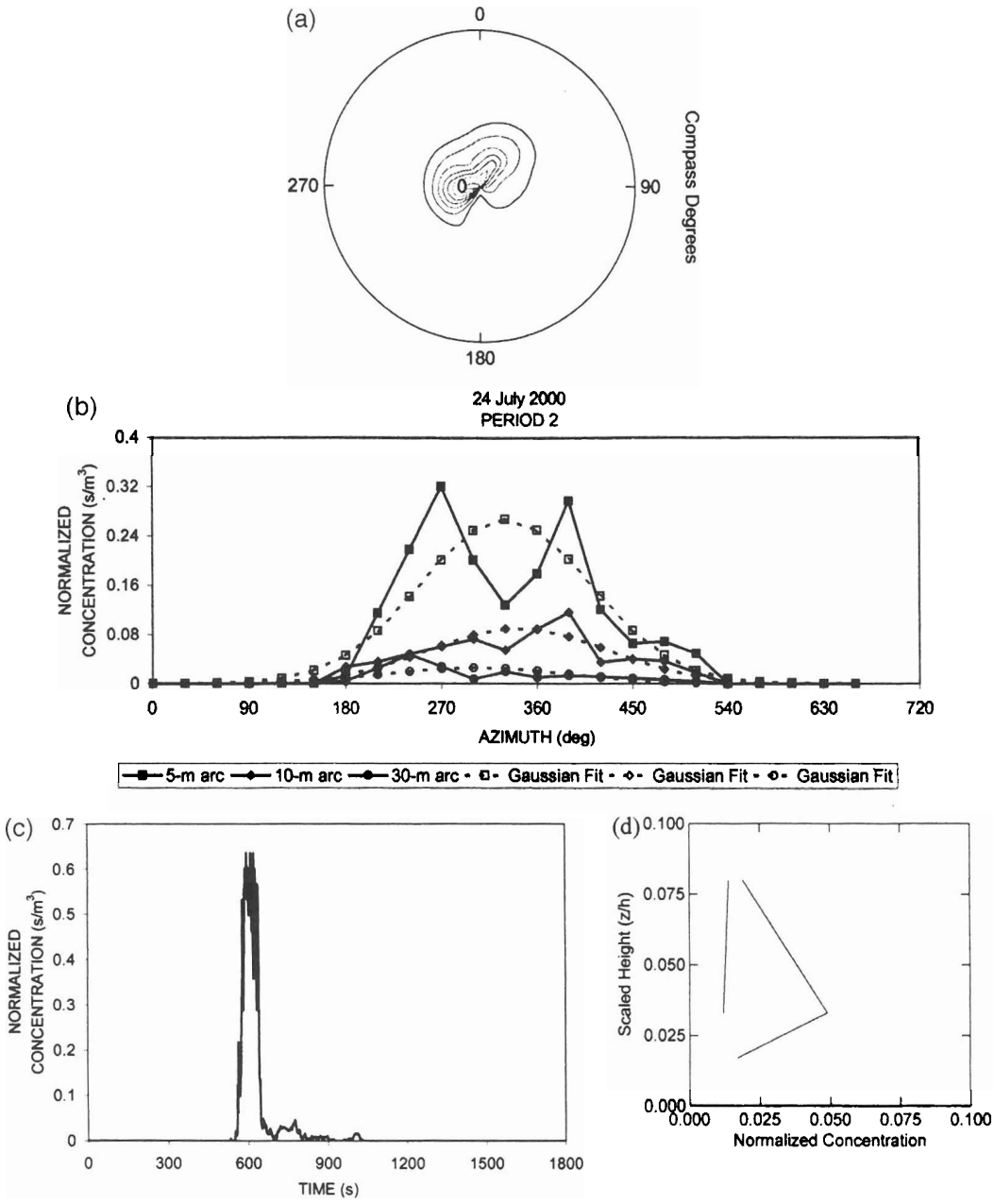

Figure 8. July 24, 2000, 7:00 am case study. Lodgepole pine canopy. (a) Spatial isopleths of 30-minute χ/Q, with the maximum contour at χ/Q = 0.5 and the tracer source at the center. Sampler positions are designated. (b) Linearized cross sections of 30-minute χ/Q compared with best-fit Gaussian cross sections. (c) High-frequency time series composed of 1 Hz averages of tracer χ at one point on the 10-m sampler arc. (d) Vertical profiles of 30-minute χ/Q at the 5-m sampler arc.

apparent in the bimodal appearance of the linearized cross section (Figure 8b). In this case, the plume has extended in two directions almost 180° opposed. The high-frequency trace (Figure 8c) shows a fairly stationary plume that meandered past the sensor fairly leisurely as the sensor indicates the plume presence for 90 seconds with a peak-to-mean ratio of 28. The bimodal appearance of this graph reflects the shifting of wind direction, as a very low velocity downslope flow is replaced by a regional mean upslope flow in the opposite direction as mesoscale heating of the surface occurs, although it is only starting to be indicated in the mean statistics near the bottom of the canopy. In the lodgepole pine data set, some near-field vertical profile data are available (Figure 8d). Two profiles are shown; again, these profiles are at fixed points, so they may miss the plume centerline, but they do indicate that even at the 5-m arc, some material is moving upward as the plume meanders in three dimensions.

Lodgepole Pine Canopy, 10:30 am, July 24, 2000

This period was characterized by markedly lower χ/Q values than earlier in the same day. Heat flux, temperature, and wind speed all increased, although *Ri* was less negative. Figure 9a shows an elongated plume with a NW-SE axis;

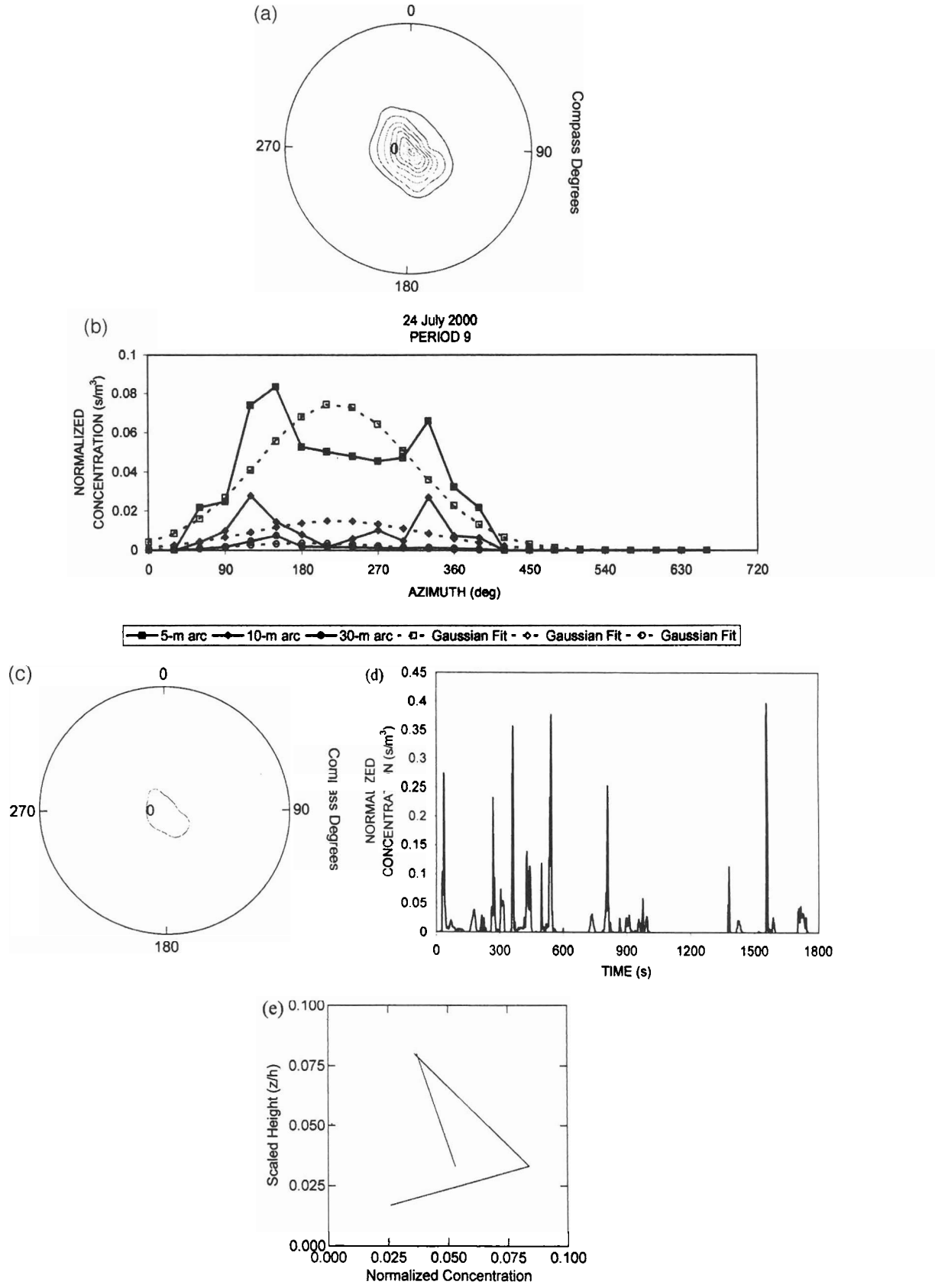

Figure 9. July 24, 2000, 10:30 am case study. Lodgepole pine canopy. (a) Spatial isopleths of 30-minute χ/Q, with the maximum contour at χ/Q = 0.125 and the tracer source at the center. Sampler positions are designated. (b) Linearized cross sections of 30-minute χ/Q compared with best-fit Gaussian cross sections. (c) Spatial isopleths of 30-minute χ/Q, scaled as Figure 8a, and the tracer source at the center. Sampler positions are designated. (d) High-frequency time series composed of 1 Hz averages of tracer χ at one point on the 10-m sampler arc. (e) Vertical profiles of 30-minute χ/Q at the 5-m sampler arc.

this same shape is also indicated by Figure 9b, as the linearized cross sections at 5 and 10 m show a distinctly bimodal distribution. To emphasize the difference in the dispersive environment between the previous case at 7:00 am and this case at 10:30 am, Figure 9c shows the same isopleth field scaled as the 7:00 am case to illustrate how much lower the χ/Q values are. The high-frequency series (Figure 9d) is remarkably different than in the 7:00 am case (Figure 8c). The series now shows the filament(s) crossing the sensor numerous times, indicating an increase in the meandering frequency or lateral wander. Although the peak-to-mean ratio was 31.6 and similar to the earlier series, it is seen that the nature of plume meander has changed. The 5-m arc vertical profiles (Figure 9e) show very similar shape to those shown in Figure 8d, although the values of χ/Q are actually higher on these profiles. Because Figures 8d and 9e illustrate data from the same day, the vertical data are from the same locations. These profiles were not on the plume centerline in these tests, but χ/Q is greater in Figure 9e because the filaments are wandering more widely. The plume in the 7:00 am case, although more concentrated, did not cross these vertical profiles as often as the more dilute plume later in the day. Furthemore, it is expected that the vertical wafting of the plume would be less in the stable early morning and more later, thus accounting for the higher elevated values of χ/Q at height shown in Figure 9e.

Ponderosa Pine Canopy, 11:00 am, June 21, 2001

Relatively high heat flux and the highest values of wind speed and *Ri* seen in these case studies characterized this period. These values would typically indicate a highly dispersive environment but the values of χ/Q are not extremely low. The isopleth plot (Figure 10a) shows the plume moved in a dominant direction and spread downwind in a relatively Gaussian pattern. The linearized cross sections show a bimodal distribution at 5 m shifting to a unimodal distribution at 10 m. Both arcs show clear maxima, indicating the plume moved in one direction much of this period. The high-frequency trace of concentration (Figure 10c) confirms this. These measurements taken SW of the tracer source show at least six peaks of similar concentration pass across the sensor, and the sensor is in the plume 44% of the time although obviously not always on the centerline. Vertical profiles are shown for both the 5 and 10-m arcs (Figure 10, d and e, respectively). These graphs indicate substantial vertical mixing of the plume as significant tracer is seen at 0.07 z/h on one profile on the 5 and 10-m arcs, although concentrations are low at the 0.2 z/h level. It is expected that vertical mixing would occur with strongly negative *Ri*, indicating hotter conditions in the lower canopy than above.

The multiple, similar magnitude peaks seen in the high-frequency series (Figure 10c) offer an opportunity to calculate the cross plume width of this plume on the 10-m arc. Because the sonic anemometers yield a three-dimensional flow field at 10 Hz, the residual lateral velocity (V) after vector rotation is available to calculate lateral plume velocity

$$P_w = P_c V \quad (3)$$

where P_w is plume width (m) and P_c is plume crossing time (s). Various assumptions go into this calculation because the peaks are often not completely discrete, and there is no reason to believe the plume moves evenly across the sampler port; it may slow down, linger, elevate slightly, and so forth. However, the first two plume crossings in this series are relatively discrete with sharp peaks, and P_c is 49 and 55 seconds, respectively; this yields P_w of 2.2 and 2.4 m.

Conclusions

Pheromone plume movement and dispersion are shown to be dependent on the ambient mixing environment. Wind speed and the state of atmospheric stability through the canopy are critical to plume movement. Mean statistics indicate that the amount and frequency of wander by narrow filamentous plumes with remarkably discrete edges are a function of both wind speed and stability. It is shown that when the surface layer is stable, the tracer plume remains relatively concentrated and shows consistency in direction due to the suppression of turbulent mixing in the stable layer. This suppressed mixing is observed even when wind speed increases if the layer remains stable, as in a shallow drainage flow. The plume filaments, measured through higher frequency sampling, show increased wander as the atmospheric boundary layer becomes unstable; this imparts a lower concentration to the mean plumes as the filaments are at a given sampling point for less time.

This study focuses on the near field (within 30 m of the source). It is recognized that plume wander will be caused by turbulent scales larger than the plume (external scales), and smaller (internal) scales will control the spread of the filament. In this study, the primary observed change in plume filament behavior is in the frequency and range of the plume wander as the mixing environment changes. The plume is widening over the short transit distances measured here, and it is expected that as the plume filament broadens downwind, larger external scales become internal and plume spreading becomes increasingly important.

It is apparent from the data collected here that in-canopy environments are often low velocity and that pheromone plumes therefore often exist in low-velocity environments. Although plume transport shows strong dependence on stability, the mixing environment in the two coniferous canopies changes slowly as solar radiation penetrates the canopy during the morning transition and does not shift dramatically until larger-scale convection generated in the deeper convective layer typical of later morning occurs. The stable atmospheric layer typical of predawn on clear nights can generate local flows that will transport a gaseous plume in a relatively concentrated fashion. These data also show that gas released in the canopy trunk space can be vented out of the top of the canopy, even in the near field. This does not appear to happen in strongly stable conditions but is not limited to strongly unstable conditions when vertical mixing is known to be strongest. In the oak-hickory canopy, there was regular near-field, canopy top venting in neutral to moderately unstable conditions and very low wind speeds.

Although three data sets are insufficient to build a strong

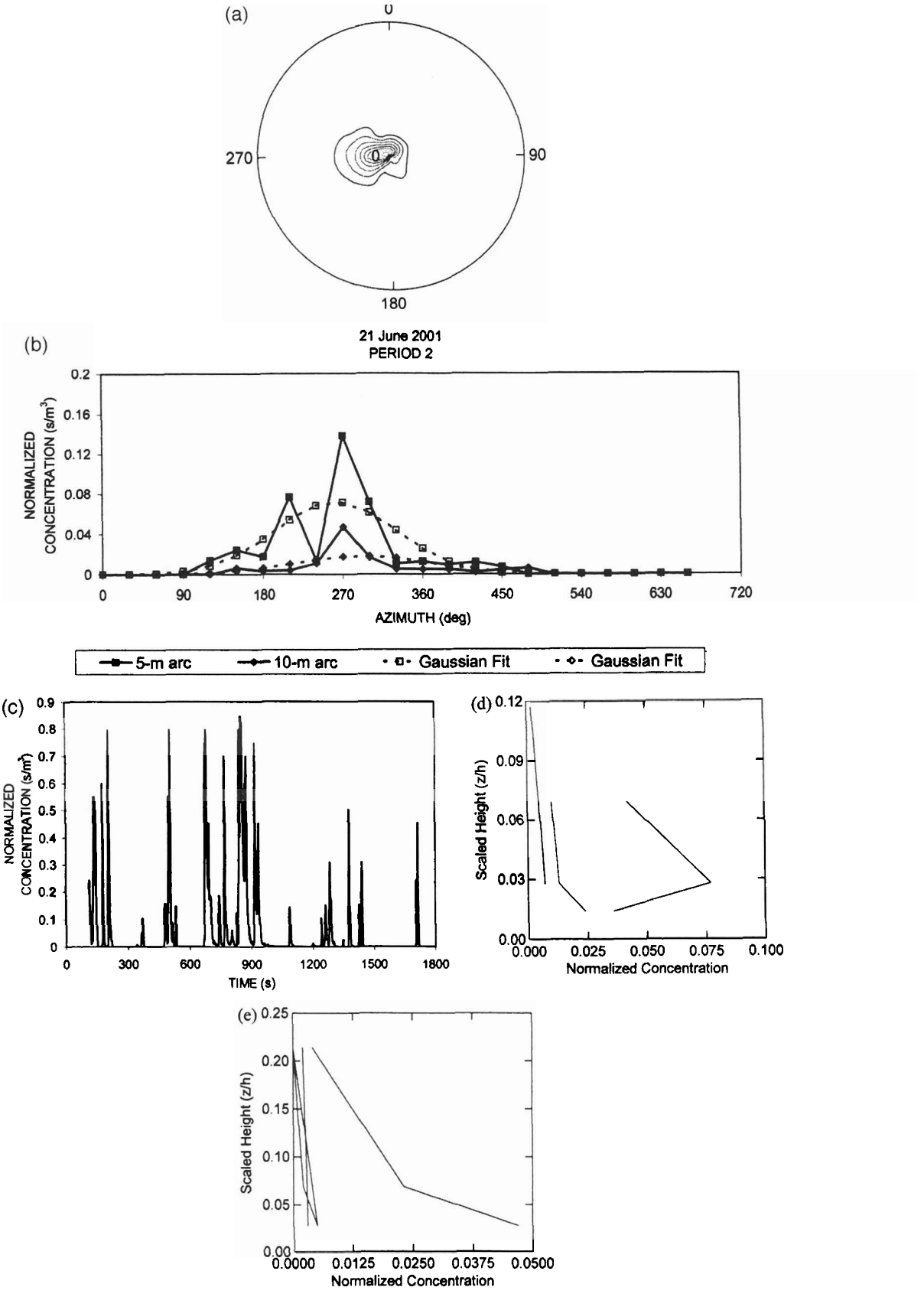

Figure 10. June 21, 2001, 11:00 am case study. Ponderosa pine canopy. (a) Spatial isopleths of 30-minute χ/Q, with the maximum contour at $\chi/Q = 0.2$ and the tracer source at the center. Sampler positions are designated. (b) Linearized cross sections of 30-minute χ/Q compared with best-fit Gaussian cross sections. (c) High-frequency time series composed of 1 Hz averages of tracer χ at one point on the 10-m sampler arc. (d) Vertical profiles of 30-minute χ/Q at the 5-m sampler arc. (e) Vertical profiles of 30-minute χ/Q at the 10-m sampler arc.

relationship between canopy architecture and the in-canopy dispersive regime, simple preliminary relationships using stems per area are shown (Figure 5). It is certain that denser canopies provide a lower velocity environment in their lower reaches that can be decoupled from the overlying atmosphere. Denser canopies may resist both the forming of shallow inversions during clear sky nocturnal conditions as well as penetration by convective mixing. It is clear that a shaded canopy sublayer can develop a temperature inversion on clear days, but at least in the ponderosa pine and lodgepole pine trials presented here, this layer was overcome by vigorous mixing of the convective boundary layer, and the plume activity was characteristic of an unstable mixing layer.

Some implications of these ideas to bark beetle plume tracking can be envisioned. The success in finding a plume (encounter probability) will be higher in unstable conditions typical of late morning to late afternoon as the filamentous plume wanders more widely. The plume remains more concentrated with more directional consistency in stable environments typical of dusk to 1 or 2 hours past dawn in the warm season. These conditions provide favorable conditions for long-range detection. These data indicate that gas released in the trunk space will, at least occasionally, emerge from the canopy close to the source. This may provide a mechanism for first attacking bark beetles to attract others. The fine structure of these plumes at high frequency has been observed previously and is confirmed here. The discrete edges of the plumes favor a digital tracking model where the insect is either in or out of the plume and perhaps encounters the plume and turns upwind (anemotactic response), only recasting when the plume is lost and turning upwind again on finding the plume (see Carde and Minks [1997] for discussions of tracking mechanisms).

A given canopy type will have characteristic mixing regimes. For instance, low-velocity, high-humidity environments in Aug. characterize the oak-hickory trunk space in the central Appalachians. Fluctuations in trunk space stability are dampened by the relatively closed structure of the canopy and the high opacity of the atmosphere due to water vapor and other biogenic emission. This causes canopy plume dispersion to be slow and relatively consistent across the diurnal period. This contrasts with a lodgepole pine stand in the northern Rockies in July that experiences large diurnal swings in humidity, temperature, stability, and even wind speed, causing dramatic differences in the in-canopy dispersive environment. It is expected that trunk space insect communities would evolve in concert with these dispersive environments and that insect activity would reflect the local dispersive regime.

Literature Cited

ALLWINE, K.J., B. LAMB, AND R. ESKRIDGE. 1992. Wintertime dispersion in a mountainous basin at Roanoke, Virginia: Tracer study. J. Appl. Meteorol. 31:1295–1311.

ALLWINE, K.J., J.H. SHINN, G.E. STREIT, K.-L. CLAWSON, AND M. BROWN. 2002. Overview of URBAN 2000: A multiscale field study of dispersion through an urban environment. Bull. Am. Meteorol. Soc. 83:521–536.

AMMAN, G.D. 1993. Potential of verbenone for reducing lodgepole and ponderosa pine mortality caused by mountain pine beetle in high-value situations. P. 33–38 *in* Proceedings of the symposium on management of western bark beetles with pheromones: Research and development, Shea, P.J. (tech. coord). USDA For. Serv. Gen. Tech. Rep. PSW-GTR-150.

AYLOR, D., J. PARLANGE, AND J. GRANETT. 1976. Turbulent dispersion of disparlure in the forest and male gypsy moth response. Environ. Entomol. 5:1026–1032.

BENNER, R.L., AND B. LAMB. 1985. A fast response continuous analyzer for halogenated atmospheric tracers. J. Atmos. Ocean. Tech. 2:582–589.

BORDEN, J.H. 1995. From identifying semiochemicals to developing a suppression tactic: A historical review. P. 3–10 *in* Proc. of the National Entomological Society of America meeting: Application of semiochemicals for management of bark beetle infestations, Salom, S.M., and K.R. Hobson (eds.). USDA For. Serv. Gen. Tech. Rep. INT-GTR-318.

CARDE, R.T., AND A.K. MINKS, EDS. 1997. Insect pheromone research: New directions. Chapman and Hall, International Thomson Publishing, New York, NY. 364 p.

CARDE, R.T., R.T. STATEN, AND A. MAFRA-NETO. 1998. Behaviour of pink bollworm males near high-dose, point sources of pheromone in field wind tunnels: Insights into mechanisms of mating disruption. Entomol. Exp. Appl. 89:34–46.

DODDS, K.J., AND D.W. ROSS. 2002. Sampling range and range of attraction of *Dendroctonus pseudotsugae* pheromone-baited traps. Can. Entomol. 134:343–355.

ELKINTON, J., R. CARDE, AND C. MASON. 1984. Evaluation of time-average dispersion models for estimating pheromone concentration in a deciduous forest. J. Chem. Ecol. 10:1081–1108.

FARES, Y., P.J.H. SHARPE, AND C.E. MAGNUSON. 1980. Pheromone dispersion in forests. J. Theor. Biol. 84:335–359.

FARRELL, J.A., J. MURLIS, X. LONG, W. LI, AND R.T. CARDE. 2002. Filament based atmospheric dispersion model to achieve short time-scale structure of odor plumes. Environ. Fluid Mech. 2:143–169.

FINNIGAN, J. 2000. Turbulence in plant canopies. Ann. Rev. Fluid Mech. 32:519–571.

GUENTHER, A., B. LAMB, AND G. ALLWINE. 1990. Building wake dispersion at an Arctic industrial site. Atmos. Environ. 24A:2329–2347.

HOLSTEN, E.H., W. WEBB, P.J. SHEA, AND R.A. WERNER. 2002. Release rates of methylcyclohexenone and verbenone from bubble cap and bead releasers under field conditions suitable for management of bark beetles in California, Oregon, and Alaska. USDA For. Serv. Res. Pap. PNW-RP-544. 21 p.

HOLSTEN, E.H., P.J. SHEA, AND R.R. BORYS. 2003. MCH released in a novel pheromone dispenser prevents spruce beetle, Dendroctonus rufipennis (Coleoptera: Scolytidae), attacks in south-central Alaska. J. Econ. Entomol. 96:31–34.

KAIMAL, J.C. 1973. Turbulence spectra, length scales and parameters in the stable layer. Bound. Layer Meteorol. 4:289–309.

KAIMAL, J.C., J.C. WYNGAARD, D.A. HAUGEN, O.R. COTE, Y. IZUMI, S.J. CAUGHEY, AND C.J. READINGS. 1976. Turbulent structure in the convective boundary layer. J. Atmos. Sci. 33:2152–2169.

KAIMAL, J.C., AND J.J. FINNIGAN. 1994. Flow over plant canopies. P. 66–108 *in* Atmospheric boundary layer flows: Their structure and measurement. Oxford University Press, New York, NY.

KRASNEC, J., D. DEMARAY, B. LAMB, AND R. BENNER. 1984. Automated sequential syringe sampler for atmospheric tracer studies. J. Atmos. Ocean. Tech. 1:372–378.

LAW, B.E., S. VAN TUYL, A. CESCATTI, AND D.D. BALDOCCHI. 2001. Estimation of leaf area index in open-canopy ponderosa pine forests at different successional stages and management regimes in Oregon. Agric. For. Meteorol. 108:1–14.

LECLERC, M.Y., N. MESKHIDZE, AND D. FINN. 2003a. Comparison between measured tracer fluxes and footprint model predictions over a homogenous canopy of intermediate roughness. Agric. For. Meteorol. 117:145–158.

LECLERC, M.Y., A. KARIPOT, T. PRABHA, G. ALLWINE, B. LAMB, AND H.L. GHOLZ. 2003b. Impact of non-local advection on flux footprints over a tall forest canopy: A tracer flux experiment. Agric. For. Meteorol. 115:19–30.

LI, W., J.A. FARRELL, AND R.T. CARDE. 2003. Tracking of fluid advected odor plumes: Strategies inspired by insect orientation to pheromone. Adapt. Behav. 9:143–170.

MAFRA-NETO, A., AND R.T. CARDE. 1994. Fine-scale structure of pheromone plume modulates upwind orientation of flying moths. Nature 369:142–144.

MURLIS, J., AND C. JONES. 1981. Fine scale structure of odour plumes in relation to insect orientation to distance pheromone and other attractant sources. Physiol. Entomol. 6:71–86.

PETERSON, H., AND B. LAMB. 1992. Comparison of the results from a meandering plume model with measured atmospheric tracer concentrations in fluctuations. J. Appl. Meteorol. 31:553–564.

PETERSON, H., AND B. LAMB. 1995. An investigation of instantaneous diffusion and concentration fluctuations. J. Appl. Meteorol. 34:2724–2746.

SCHLYTER, F. 1992. Sampling range, attraction range, and effective attraction radius: Estimates of trap efficiency and communication distance in coleopteran pheromone and host attractant systems. J. Appl. Entomol. 114:439–454.

SHEA, P.J., M.D. MCGREGOR, AND G.E. DATERMAN. 1992. Aerial application of verbenone reduces attack of lodgepole pine by mountain pine beetle. Can. J. For. Res. 22:436–441.

STAEBLER R.M. 2003. Forest sub-canopy flows and micro-scale advection of carbon dioxide'. Ph.D. dissertation, State University of New York, Albany, NY. 170 p.

STRAND T., B. LAMB, G. ALLWINE, H. PETERSON, H. THISTLE, E. HOLSTEN, AND P. SHEA. 2002. Pheromone fate and transport in forest canopies. Extended abstract, P. 1.6 *in* Proc. of the 25th conference on agricultural and forest meteorology. American Meteorological Society, Boston, MA.

THISTLE, H.W., D.R. MURRAY, M.R. RATTE, AND M.R. CARROLL. 1995. Atmospheric tracer concentrations from an elevated source in an urban core. J. Environ. Eng. 121:5–15.

THISTLE, H.W., P. SHEA, E. HOLSTEN, AND D. QUILICI. 1999. Pheromone dispersion in the canopy trunk space: Analysis of plume data. Am. Soc. Agric. Eng. Tech. Pap. # 99–1013, St. Joseph, MI.

THISTLE, H.W. 2000. The role of stability in fine droplet dispersion. Trans. Am. Soc. Agric. Eng. 43:1409–1413.

THISTLE, H.W., H. PETERSON, B. LAMB, T. STRAND, G. ALLWINE, E. HOLSTEN, AND P. SHEA. 2002. Mass balance of pheromone surrogate plumes in the canopy trunk space. Am. Soc. Agric. Eng. Tech. Pap. #021006, St. Joseph, MI.

THROOP, W., H. THISTLE, AND R. BECKLEY. 2001. Leaf area measurements in four forest canopies using a plant canopy analyzer and hemispherical photography. Am. Soc. Agric. Eng. Tech. Pap. #01–8020, St. Joseph, MI.

TURCHIN, P., AND F.J. ODENDAAL. 1996. Measuring the effective sampling area of a pheromone trap for monitoring population density of southern pine beetle (Coleoptera: Scolytidae). Environ. Entomol. 25:582–588.

WERNER, R.A., AND E.H. HOLSTEN. 1995. Current status of research with the spruce beetle, *Dendroctonus rufipennis*. P. 23–29 *in* Proc. of the National Entomological Society of America meeting: Application of semiochemicals for management of bark beetle infestations, Salom, S.M., and K.R. Hobson (eds.). USDA For. Serv. Gen. Tech. Rep. INT-GTR-318.

WILCZAK, J.M., S.P. ONCLEY, AND S.A. STAGE, 2001. Sonic anemometer tilt correction algorithms. Bound. Layer Meteorol. 99:127–150.

YEE, E., R. CHAN, P.R. KOSTENIUK, G.M. CHANDLER, C.A. BILTOFT, AND J.F. BOWERS. 1994. Experimental measurements of concentration fluctuations and scales in a dispersing plume in the atmospheric surface layer obtained using a very fast response concentration detector. J. Appl. Meteorol. 33: 996–1016.